Journal of Biomechanics 197 (2026) 113169

Contents lists available at ScienceDirect

Journal of Biomechanics

journal homepage: www.elsevier.com/locate/jbiomech

Comparative tensile properties of the equine vagina, penile sheath, and scrotum

Angel E. Collins[a], Jennifer S. Wayne[b], Cecile A. Ferrando[c], Raffaella De Vita[a,*]

[a] STRETCH Lab, Department of Mechanical Engineering, Virginia Tech, 330A Kelly Hall, 325 Stanger Street, Blacksburg, VA 24061, United States
[b] Department of Biological Systems Engineering, Virginia Tech, 305 Seitz Hall, 155 Ag Quad Lane, Blacksburg, VA 24061, United States
[c] Division of Urogynecology & Reconstructive Pelvic Surgery, Department of Obstetrics & Reproductive Sciences, University of California San Diego, 9500 Gilman Drive, La Jolla, CA 92037, United States

HIGHLIGHTS

- Uniaxial tensile testing was performed on male and female equine genital tissues, with strain quantified using digital image correlation.
- Tissue specimens were excised and aligned circumferentially around the vaginal lumen, penile shaft, and scrotal contour.
- Vaginal and scrotal tissues showed comparable tangent moduli, while the penile sheath exhibited a significantly lower tangent modulus.

GRAPHICAL ABSTRACT

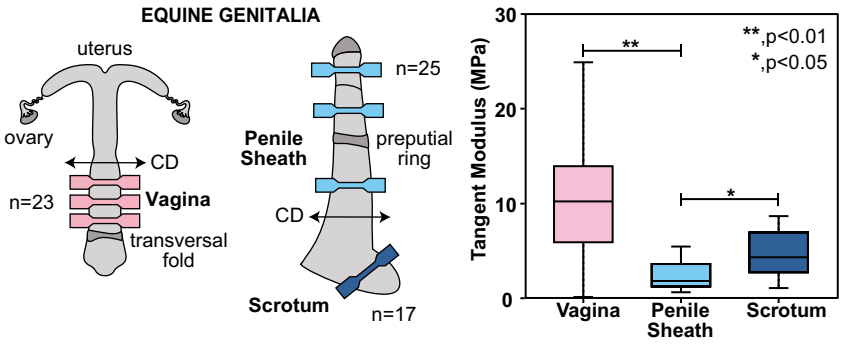

ARTICLE INFO

Keywords:
Vagina
Penile sheath
Scrotum
Equine
Mechanical properties

ABSTRACT

This experimental study characterizes the elastic behavior of male and female equine genital tissues using uniaxial tensile testing, with strain measurements obtained via digital image correlation. Dog-bone-shaped tissue specimens were excised from mares and geldings (n = 23 from female specimens and n = 42 from male specimens) with all specimens aligned along the circumferential direction (CD) of the vagina, penis, and scrotum. The results include load-displacement data, stress–strain data, and tangent moduli for the penile sheath, vaginal canal, and scrotum, with strain measured in both the CD and the longitudinal direction (LD). Findings indicate that vaginal and scrotal tissues exhibit comparable mechanical properties (tangent moduli: 10.16 ± 1.30 MPa for the vagina and 4.81 ± 1.66 MPa for the scrotum), whereas the penile sheath (tangent modulus: 2.30 ± 1.43 MPa) differs significantly from the vaginal and scrotal tissues ($p < 0.01$ and $p < 0.05$, respectively). This mechanical evaluation of vaginal, penile, and scrotal tissues has implications for advancing surgical techniques, developing genital prostheses, and informing biomechanical models of the pelvic region.

1. Introduction

Sex-based disparities in genital research have been widely recognized across multiple disciplines, with male genitalia historically receiving greater scientific attention than their female counterparts (Ah-King et al., 2014). Within the field of biomechanics in particular, research has largely centered on theories and models related to copulation and erectile mechanisms, with a predominant focus on penile hemodynamics

* Corresponding author.
Email address: devita@vt.edu (R. De Vita).

https://doi.org/10.1016/j.jbiomech.2026.113169
Accepted 12 January 2026
Available online 16 January 2026

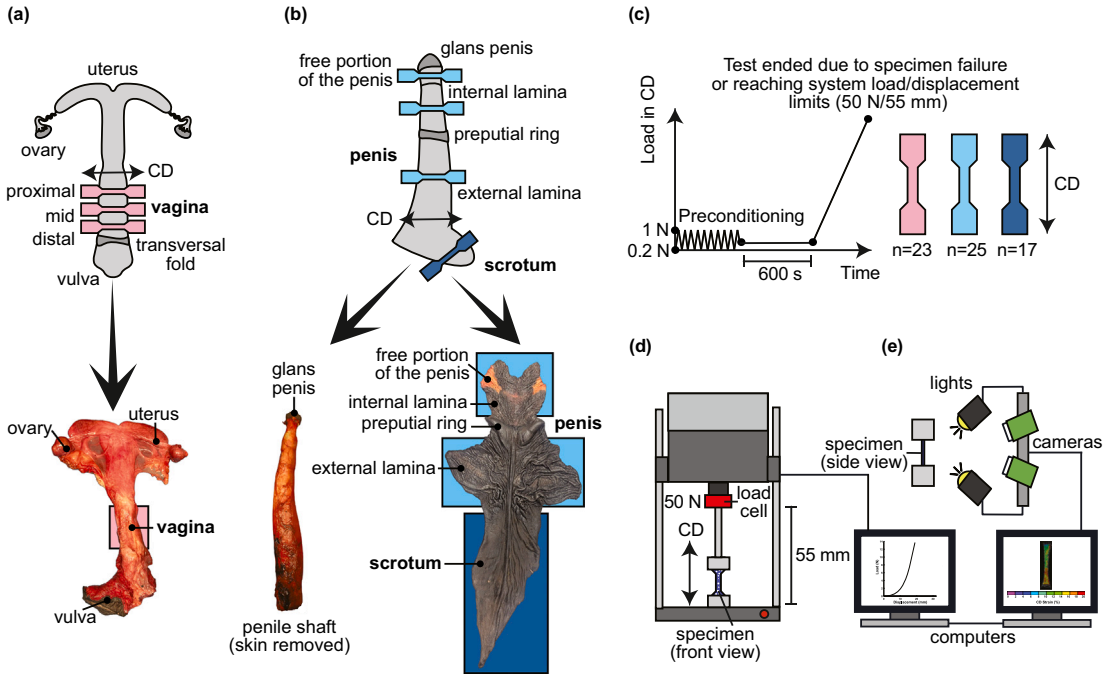

Fig. 1. Anatomical diagrams and photographs of the equine (a) vagina showing the proximal, mid, and distal regions from which tissue specimens were isolated for testing and (b) penis and scrotum illustrating the free portion of the penis, the prepuce (internal and external laminae), and the scrotal tissue. The photographs show the vagina and penile shaft after removal of the external skin, along with the excised skin specimens from the free portion of the penis, the prepuce, and the scrotum. (c) Experimental protocol applied to all vaginal (n = 23), penile sheath (n = 25), and scrotal (n = 17) specimens, including preconditioning (10 cycles, 0.2–1 N at 0.1 mm/s), a 600 s resting period, and tensile loading at 0.4 mm/s until a termination criterion was reached: a 20% load drop, the 55 mm actuator stroke limit, or the 50 N load cell limit. (d) Tensile testing system equipped with a 50 N load cell and a 55 mm actuator stroke limit, shown with a mounted specimen. (e) View of the test region exposed to the cameras for DIC strain measurements. All specimens were loaded in the circumferential direction (CD) of the organs.

and structural responses (Udelson et al., 1998a,b,c; Frohrib et al., 1987). Copulation involves significant mechanical deformation of external and internal genital structures, beginning with the engorgement and stiffening of erectile tissue and continuing through the compressive and tensile forces exerted on the penis and vaginal canal during intromission and thrusting. Although research on genital evolution is steadily increasing for both sexes, aside from theories related to copulation mechanisms (Langerhans et al., 2016), the biomechanical properties of both male and female genitalia remain largely understudied.

In most mammals, the vagina can accommodate changes in shape and pressure, such as those necessary in sexual intercourse and childbirth, due to its distensibility and compliance (Dubik et al., 2025). The vaginal wall is composed of the mucosa, muscularis, and adventitia layers, enabling it to undergo substantial stretching from its resting diameter and subsequently recover without permanent deformation. In contrast, the penis must achieve a biomechanical balance between rigidity and expansion to maintain functional erection during sexual intercourse (Gefen et al., 1999; Timm et al., 2005). During functional erection, the corpora cavernosa and corpus spongiosum engorge with blood, and the tunica albuginea supports rigidity. This dual requirement is facilitated by the distensibility of the entire external covering of the penis, the penile sheath. The elasticity of the penile sheath is responsible for its protective, adaptive, and mobile functions, enhancing tissue resilience during erection and copulatory activity (Foster, 2016). Finally, scrotal tissue also exhibits high compliance and elasticity, facilitating mobility that protects the testes from mechanical stress and helps maintain thermoregulatory function (Waites, 1991).

In addition to advancing our understanding of genital evolution and copulatory function, the biomechanical properties of male and female genitalia can support the development of treatment strategies for a wide range of clinical conditions, injuries, and pathologies. These include pelvic organ prolapse (de Landsheere et al., 2016; Epstein et al., 2007; Jean-Charles et al., 2010; Lei et al., 2007), vaginal agenesis (McQuillan and Grover, 2014), vaginal atrophy (Epstein et al., 2008), Peyronie's disease (Gefen et al., 2002; Stuntz et al., 2016), penile and scrotal degloving injuries (Alkahtani et al., 2020), and erectile dysfunction (Lue, 2000), among others. These conditions alter the mechanical behavior of genital tissues, and quantification of properties such as stiffness and tensile strength can directly inform surgical planning, prosthetic design, and tissue engineering approaches.

Biomechanical studies of the genitalia are most commonly performed using animal tissues, as these models typically yield specimens of sufficient size and geometry (e.g., standardized dog-bone shapes) for reliable mechanical testing and material characterization. In contrast, human genital tissues are significantly more difficult to study due to ethical constraints and limited availability. Several large animal models have been utilized to investigate the biomechanical properties of vaginal tissue (Dubik et al., 2025), with swine (McGuire et al., 2019; Pack et al., 2020) and ewes (Rynkevic et al., 2017) among the most frequently used due to their physiological and structural similarities to human vaginal tissue. The vaginal tissue in these species is composed of the same fundamental structural components, such as collagen, elastin, and smooth muscle (McCracken et al., 2021). Recently, equines have been used to characterize the mechanical behavior of male genital tissues (Bose et al., 2024), as their external, non-retractable penile tissue and visible scrotum share anatomical characteristics with humans (Khorshidi et al., 2024). Both male horses and humans possess musculocavernous penises, comprising paired corpora cavernosa and a single corpus spongiosum that engorge with blood during erection (Budras et al., 2012). This engorgement likely generates comparable physiological forces on surrounding tissues, including the penile sheath and scrotum.

While species-specific differences in penile dimensions are acknowledged, previous literature has cited notable anatomical similarities between equine and human genitalia, making the equine model relevant

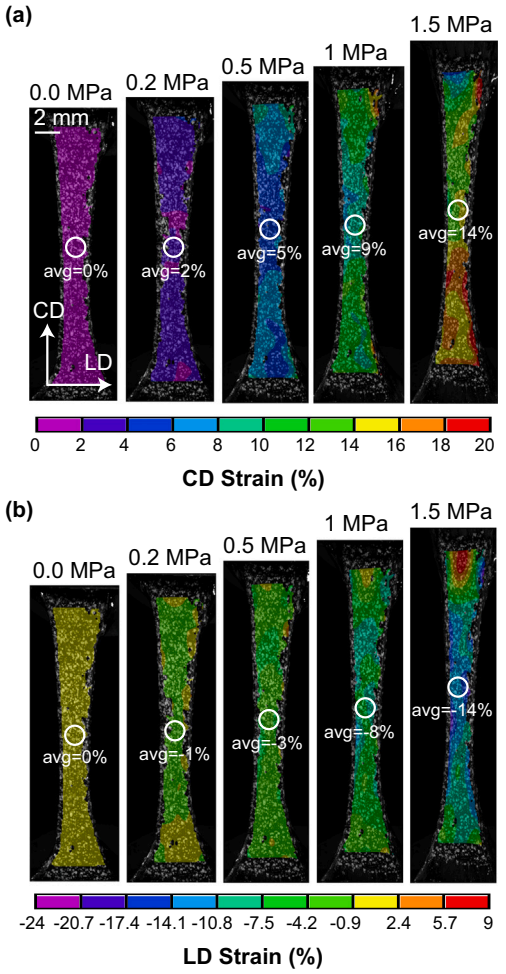

Fig. 2. Strain maps in (a) CD and (b) LD at increasing values of the axial stress applied in CD for one representative (vaginal) specimen.

for genital tissue research. Specifically, the equine model has been employed in ovarian studies (Adams et al., 2012), as well as in research on fertility (Carnevale, 2008), reproductive technologies (Benammar et al., 2021), and erectile dysfunction in stallions (Bose et al., 2024). Thus, the equine model is a promising candidate for comparative studies of genital tissues, including the vagina, penile sheath, and scrotum.

This study quantified the deformation behavior of the equine vaginal wall, penile sheath, and scrotum using uniaxial tensile testing combined with digital image correlation (DIC) for strain measurement. Specimens were loaded in the circumferential direction (CD), with strain measured both along the CD and perpendicular to the loading axis. The results provide the first comparative mechanical characterization of genital tissues. Studies like this inform evolutionary analyses of reproductive morphology and copulatory mechanics across species, while also offering translational relevance for tissue engineering and regenerative medicine. The mechanical data collected have important implications for surgical reconstruction, particularly for tissue selection and graft design in genital reconstructive procedures.

2. Methods

2.1. Specimen preparation

This study was conducted with the approval of the Institutional Animal Care and Use Committee (IACUC) at Virginia Tech. Reproductive organs from two adult mares (one nulliparous and one previously bred, though the exact number of prior pregnancies was not documented) and two adult geldings were obtained from the Virginia Tech Middleburg Agricultural Research and Extension Center (Fauquier County, Virginia).

Table 1
Mean (± S.D.) geometric measurements of dog-bone-shaped specimens from the vagina, penile sheath, and scrotum.

Region	Thickness (mm)	Width (mm)	Gauge length (mm)	CSA (mm^2)
Vagina (n = 23)				
Proximal	2.67 ± 0.61	4.18 ± 0.61	38.96 ± 0.24	11.40 ± 3.30
Mid	2.24 ± 0.63	4.09 ± 1.34	38.09 ± 2.06	9.72 ± 3.25
Distal	2.59 ± 0.97	4.10 ± 1.43	35.39 ± 1.93	15.78 ± 4.71
Average	**2.74 ± 0.72**	**4.36 ± 1.29**	**38.49 ± 2.09**	**11.52 ± 4.85**
Penile Sheath (n = 25)				
Free	3.27 ± 0.69	5.36 ± 0.56	33.69 ± 6.69	17.69 ± 5.13
Internal	3.37 ± 0.64	5.42 ± 0.89	39.91 ± 4.46	16.28 ± 6.44
External	3.56 ± 0.49	5.14 ± 0.69	38.17 ± 2.64	18.44 ± 4.27
Average	**3.41 ± 0.60**	**5.33 ± 0.78**	**38.45 ± 4.84**	**17.06 ± 5.70**
Scrotum (n = 17)				
Scrotum	2.66 ± 0.54	5.45 ± 1.28	37.30 ± 3.05	14.62 ± 4.80

In mares, the vaginal canal was dissected from the uterus at the level of the cervix via the vaginal fornix, and from the external genitalia at the transverse fold. Using the urethra as a ventral guide, the vaginal canal was then incised longitudinally along its length. In the geldings, an incision was made at the base of the glans penis and extended caudally along the penile shaft and over the scrotum. This incision separated the skin to a plane to the level of the dartos fascia, leaving the tunica albuginea and underlying erectile tissues intact. This allowed for the removal of the skin and subcutaneous tissue covering both the penis and scrotum.

Dog-bone-shaped specimens were cut along the CD of the vaginal canal in the proximal, mid, and distal regions. Similarly, dog-bone-shaped specimens were cut along the CD of the penile sheath and scrotum (Fig. 1(a)–(b)). Due to the lack of clear anatomical demarcation within the vaginal regions and scrotum, precise regional attribution was not feasible. As a result, mid-vaginal specimens may include portions of proximal or distal tissue, and scrotal specimens may include perineal tissue. All specimens were cut using a 3D-printed punch die with the following dimensions: clamp width: 17.91 mm, necking width: 7.11 mm, and necking length: 21 mm. Tissue specimens were hydrated using phosphate-buffered saline (PBS; pH 7.4; Fisher Scientific, Hampton, NH)–soaked gauze, sealed in resealable plastic bags, and stored at −20 °C until mechanical testing. This storage step was necessary because each reproductive tract yielded a large number of specimens, and the complete dissection–preparation–testing workflow could not be performed in a single session. Freezing the tissues at −20 °C prevented degradation before testing and is a widely used approach in reproductive biomechanics when large sample sets must be processed. Prior work has shown that freezing has minimal effect on the tensile behavior of vaginal tissue (Rubod et al., 2007). All specimens in this study followed the same storage and thawing protocol, ensuring consistent treatment across groups.

2.2. Mechanical testing

For mechanical testing, the dog-bone-shaped specimens were thawed in the refrigerator at 4 °C. Once thawed, the specimens were dyed blue with an aqueous methylene blue solution (1% w/v) to darken the tissue. A high-contrast speckle pattern was applied to the tissue surface using a mesh grid and white aerosol fast-dry gloss paint (McMaster-Carr, Elmhurst, IL). Adequate time was provided for the paint to dry and adhere to the tissue surface. This speckle pattern enabled non-contact strain measurements using DIC techniques, as described by Lionello et al. (2014).

Measurements of gauge length, width, and thickness were taken for each mare and gelding specimen. Thickness measurements were

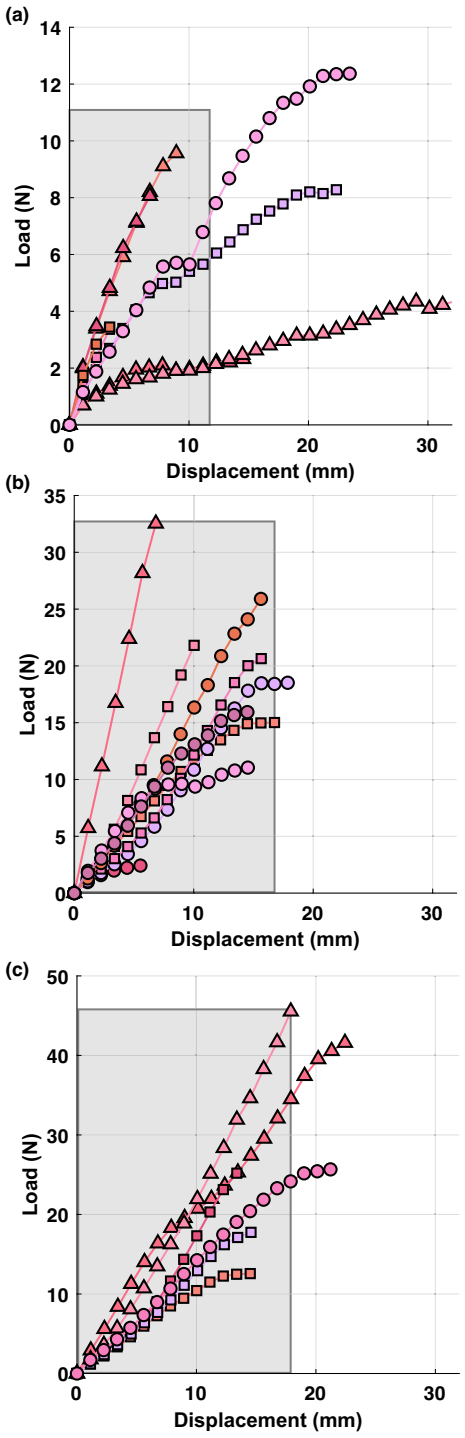

Fig. 3. Load-displacement curves for equine vaginal specimens are presented in three groups based on the maximum load they achieved: (a) below 14 N ($n = 8$), (b) below 35 N ($n = 9$), and (c) below 50 N ($n = 6$). Data from proximal, mid, and distal vaginal specimens are denoted by circles, squares, and triangles, respectively. Corresponding stress-strain curves for the load-displacement data in the shaded regions are presented in Fig. 5.

performed using a high-precision CCD laser displacement sensor (accuracy: ±0.05%, LKG82, Keyence, Inc., Japan) along the midline of the specimen's neck-to-neck length at three points, with the values averaged to determine a single thickness for each specimen. Initial length and width measurements were taken using digital calipers (accuracy: ±0.05 mm, Mitutoyo Absolute Low Force Calipers Series 573, Japan).

Speckled specimens were mounted in an ElectroPuls E1000 uniaxial testing system (Instron Corporation, Norwood, MA) equipped with a 50 N load cell (accuracy ±0.05 N) and submersible pneumatic grips rated for 250 N tension capacity. Pneumatic clamping was used to securely hold the specimen ends and minimize slippage during mechanical testing. Specifically, specimens were clamped so that the speckled mucosa layer of the vagina and the superficial fascia of the penile-scrotal flap were visible to a stereo camera system. To prevent tissue dehydration during testing, specimens were periodically sprayed with PBS.

The experimental protocol for each specimen is schematically presented in Fig. 1(c), which outlines the complete sequence of preconditioning, resting, and tensile loading steps applied identically to every specimen. Specimens were preconditioned via cyclic uniaxial loading between 0.2 N and 1 N at a displacement rate of 0.1 mm/s for ten cycles. This slower rate, lower than the test rate of 0.4 mm/s used during testing, was used to minimize tissue disruption and promote a consistent mechanical response prior to testing. The preconditioning parameters were selected following established protocols for soft biological tissues (McGuire et al., 2019) and based on preliminary testing. Additional cycles did not further change the load–displacement response, indicating that ten cycles were sufficient to achieve a repeatable mechanical state. Following preconditioning, the specimens were held at the preload-corresponding displacement for a resting period of 600 s. During this hold time, the specimen was maintained at a fixed gauge length based on specimen displacement at 0.2 N (the last preconditioning cycle). This rest interval was included because soft tissues are viscoelastic: when the specimen was held at a fixed length after preconditioning, the load decreased over time as the tissue relaxed. Allowing this stress-relaxation process to stabilize ensured that all specimens began tensile loading from comparable mechanical conditions. Following this phase, specimens were stretched at a constant displacement rate of 0.4 mm/s until one of the following failure criteria was met: (1) the actuator reached its 55 mm stroke limit, (2) the applied load exceeded the 50 N capacity of the load cell, or (3) a 20% drop in load occurred from the recorded peak value (Fig. 1(c)). Data were analyzed up to the point at which any of these conditions were met. Specimens were excluded only when full-field strain measurements could not be reliably computed, such as when the speckle pattern degraded at large stretches, moved out of the camera field of view, or when tearing occurred near the grips rather than in the gauge region. These exclusion criteria ensured that all reported mechanical data were based on valid and accurate DIC-derived strain fields. Each specimen underwent the complete preconditioning, resting, and tensile testing sequence exactly once, using the same protocol and loading parameters. In total, 65 specimens were tested (23 vaginal, 25 penile sheath, and 17 scrotal), all following the identical procedure described above.

Throughout mechanical testing, high-resolution (2468 pixels × 2065 pixels) images of the specimens were captured at a rate of 2 images per second using two CMOS cameras (Basler ace acA2440-75 µm, Basler, Inc., Exton, PA, USA) equipped with C-mount lenses (Xenoplan 2.8/50, Schneider Optics Inc., Hauppauge, NY) and rotating linear polarizers (Pro32-30.5, Edmund Optics, Barrington, NJ). Non-contact strain measurements were performed with a 3D DIC system (Vic-3D, version 9, Correlated Solutions Inc., Irmo, SC) (Fig. 1(e)). The system was calibrated before each test by capturing images of a 12 mm × 9 mm target grid with 1 mm spacing. The same imaging setup and calibration procedure were used for every specimen to maintain consistency across all tests.

2.3. Data analysis

Full-field Lagrangian strain maps were obtained using DIC, providing pointwise strain data across the surface of each tested specimen exposed to the cameras. To ensure consistency across specimens and avoid edge effects near the grips, a region of interest was selected near

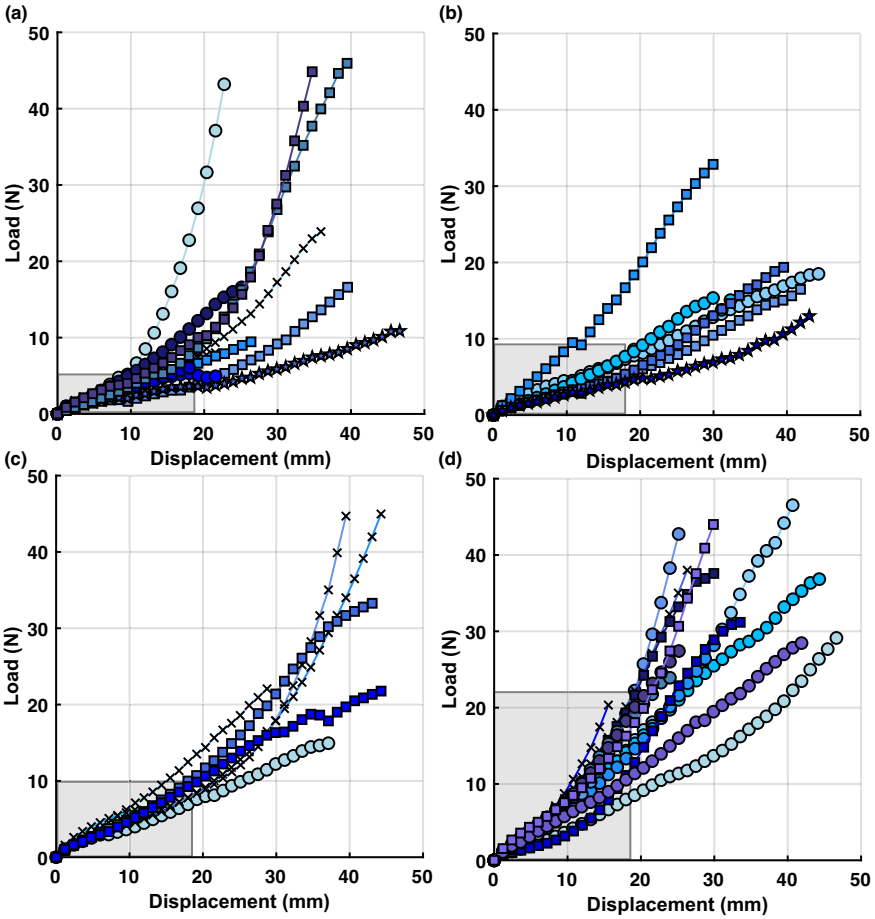

Fig. 4. Load-displacement curves for equine penile sheath and scrotum specimens are presented in four panels to reduce visual clutter; all data fall below the load cell capacity (50 N): (a) $n = 11$, (b) $n = 9$, (c) $n = 9$, and (d) $n = 13$. Data regional specimens from the free penis portion, internal lamina, external lamina, and scrotum are denoted in stars, crosses, squares, and circles, respectively. Data is presented in four panels for visibility. Corresponding stress-strain curves for the load-displacement data in the shaded regions are presented in Fig. 6.

the midsection of the gauge region for each specimen. The reported strain values represent the average of the pointwise strains within this mid-region at each load (or stress) value during testing (Fig. 2). Axial (or normal) strain was measured in two orthogonal anatomical directions: the CD, which was aligned with the loading direction, and the LD, which was oriented perpendicular to the CD. These directions are referred to, throughout this study, as "CD strain" and "LD strain," respectively. Normal stress in the CD was calculated by dividing the axial load by the corresponding cross-sectional area. This stress quantity will henceforth be referred to simply as "stress." To clearly display all curves, the load, displacement, stress, and strain data were downsampled by retaining every 20th to 30th data point, improving plot readability without compromising the overall trends.

The tangent modulus was determined from the stress–strain curves (in the CD) for each specimen. First, the stress–strain curve was smoothed using a moving average. The slope of the curve at each strain value was then computed. Only the slope-strain data after 5% strain were used to determine the linear region of the stress–strain curve. Between 5% strain and the strain measured at the end of each test, consecutive windows of 5 points were compared for slope changes and, when such changes were less than 0.5%, the maximum slope was defined as the tangent modulus.

3. Statistical analysis

Tangent modulus served as the dependent variable for the statistical analysis. For the mare or gelding, a one-way repeated measures analysis of variance (ANOVA) was performed to evaluate differences in the tangent moduli across the anatomical regions of each organ (proximal, mid, and distal vagina or free penis, internal lamina, and external lamina). Assumptions of normality, absence of significant outliers, and sphericity were evaluated. Normality was tested using the Shapiro-Wilk test, and sphericity was assessed with Mauchly's test. When Mauchly's test indicated a violation of sphericity, Greenhouse-Geisser corrections were applied. In cases where no significant difference across anatomical regions was found (e.g., proximal, mid, and distal vagina or free penis, internal lamina, and external lamina), based on the initial one-way repeated measures ANOVA, the data were pooled for comparisons of tangent moduli across main anatomical structures (e.g., vagina, penile sheath, and scrotum). When the one-way ANOVA indicated significant differences in the mean tangent moduli, post hoc pairwise comparisons were conducted. Statistical significance was set at $p < 0.05$.

4. Results

The geometric measurements of the dog-bone specimens, including thickness, width, gauge length, and cross-sectional area (CSA) for vaginal, penile, and scrotal specimens are reported in Table 1. Measurements are reported based on anatomical regions in the vagina (proximal, mid, and distal), the penile sheath (free penis, internal lamina, and external lamina) and the scrotum.

During uniaxial tensile testing, specimens typically failed through rupture at or near the center of the gauge region, consistent with the

expected localized stress concentration. In most cases, failure occurred through gradual elongation followed by delamination, a failure mode in which adjacent tissue layers in the tissues separated under shear or tensile loading before the specimen ruptured completely. This intratissue separation was readily identified in the DIC images, as delamination exposed lighter underlying tissue beneath the darkened, speckled surface. However, in some specimens, failure occurred by gradual elongation followed by sudden rupture, suggesting the tissue had reached its ultimate tensile strength. To ensure consistency in observed failure modes, specimens that exhibited a 20% drop in maximum load due to tearing near the grips were not included in the final analysis of tangent modulus, leaving a total of $n = 21$ vaginal specimens, $n = 24$ for penile specimens, and $n = 12$ scrotal specimens. Strain was continuously monitored throughout testing using DIC to enable precise, full-field strain analysis and accurate tracking of tissue deformation. As a result, stress–strain data are presented only up to the point at which reliable strain measurements were captured by the DIC system.

Figs. 3 and 4 display the load–displacement curves for all vaginal tissue specimens and for all penile and scrotal specimens, respectively, grouped by intervals of increasing maximum load. Specimens reached different maximum loads because some failed at lower forces, whereas others continued loading up to the 50 N capacity of the load cell. The curves were grouped by maximum load solely to improve figure readability. Specimens exhibited varying degrees of nonlinearity; some load–displacement curves appeared more linear than others, with slope differences observed across all tested samples. This nonlinear behavior reflects the expected changes in tissue stiffness with deformation, which is characteristic of soft biological tissues.

Figs. 5 and 6 show stress–strain curves for vaginal, penile, and scrotal specimens, grouped into subfigures by increasing maximum stress (three categories for vaginal tissue and four for the penile sheath and scrotum). The curves were grouped to improve comparability among specimens with similar stress magnitudes; using a single y-axis range would compress lower-stress curves and create visual clutter, and the full set of curves could not be presented clearly within a single figure. Separate subfigures therefore provide a clearer and more interpretable representation of the data. The stress–strain curves in Figs. 5 and 6 exhibited an initial decrease in slope with increasing strain. This behavior likely reflects rapid load accumulation during early displacement, due to the removal of slack or pre-tension in the specimen, before strain became more evenly distributed across the gauge region.

Fig. 7 shows axial strain (CD) versus transverse strain (LD) curves for vaginal specimens, grouped by the stress intervals used in Fig. 5 to enhance figure readability and facilitate comparison across curves. Similarly, Fig. 8 presents these curves for penile and scrotal specimens, grouped according to the stress intervals in Fig. 6 for the same reasons. Among the $n = 23$ vaginal tissue specimens, 14 exhibited negative transverse strain in response to axial loading, indicating contraction perpendicular to the applied load. Three specimens showed an initial increase in LD strain, suggesting transient widening, followed by a decrease. The remaining specimens exhibited LD strain that remained near zero or declined gradually. Of the $n = 42$ gelding tissue specimens, 29 similarly displayed negative transverse strain, seven showed an initial increase in LD strain before decreasing, and the rest exhibited minimal or inconsistent transverse strain behavior that could not be clearly categorized as either positive or negative.

Tangent moduli for the proximal, mid, and distal regions of the equine vagina are shown in Fig. 9(a), while Fig. 9(b) presents data for the penile sheath, including the free penis, internal lamina, and external lamina. A one-way repeated measures ANOVA revealed no significant differences in tangent modulus across vaginal regions ($p = 0.450$), and similarly, no differences were found among regions of the penile sheath ($p = 0.349$). Tangent moduli for the scrotum are shown in Fig. 9(c).

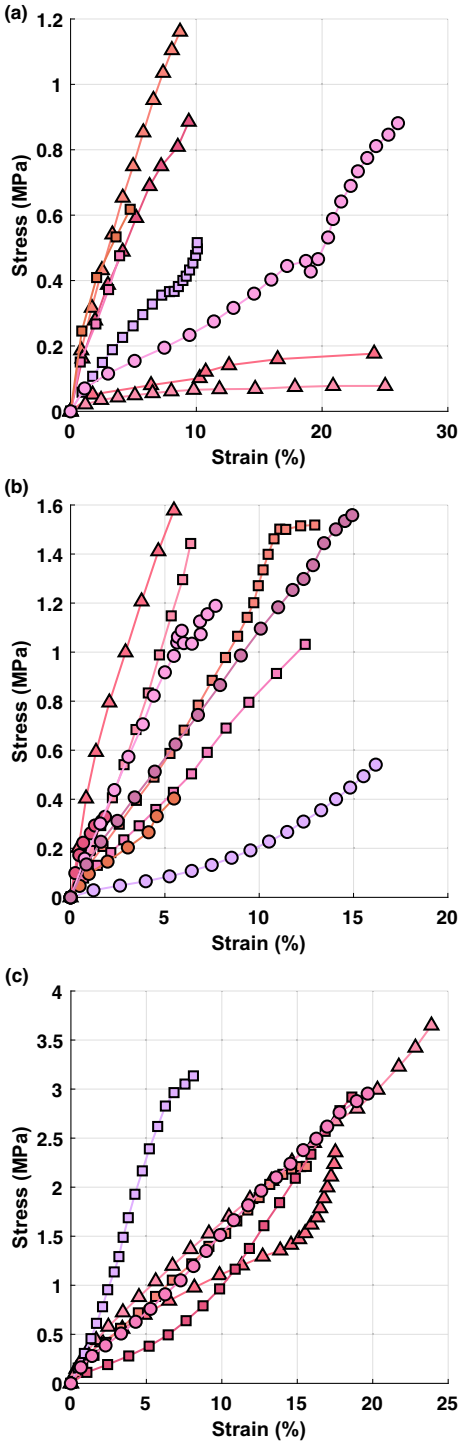

Fig. 5. Stress-strain curves for equine vaginal specimens are presented in three groups based on maximum stress achieved: (a) below 1.2 MPa ($n = 8$), (b) below 1.6 MPa ($n = 9$), and (c) below 4 MPa ($n = 6$). Data from proximal, mid, and distal vaginal specimens are denoted by circles, squares, and triangles, respectively. The same colors and symbols are used here and in Fig. 3 to represent the same specimens.

The scrotum was not subdivided, and no within-organ ANOVA was performed.

Due to the absence of regional differences, data were pooled within each organ for comparison across the main anatomical structures. A

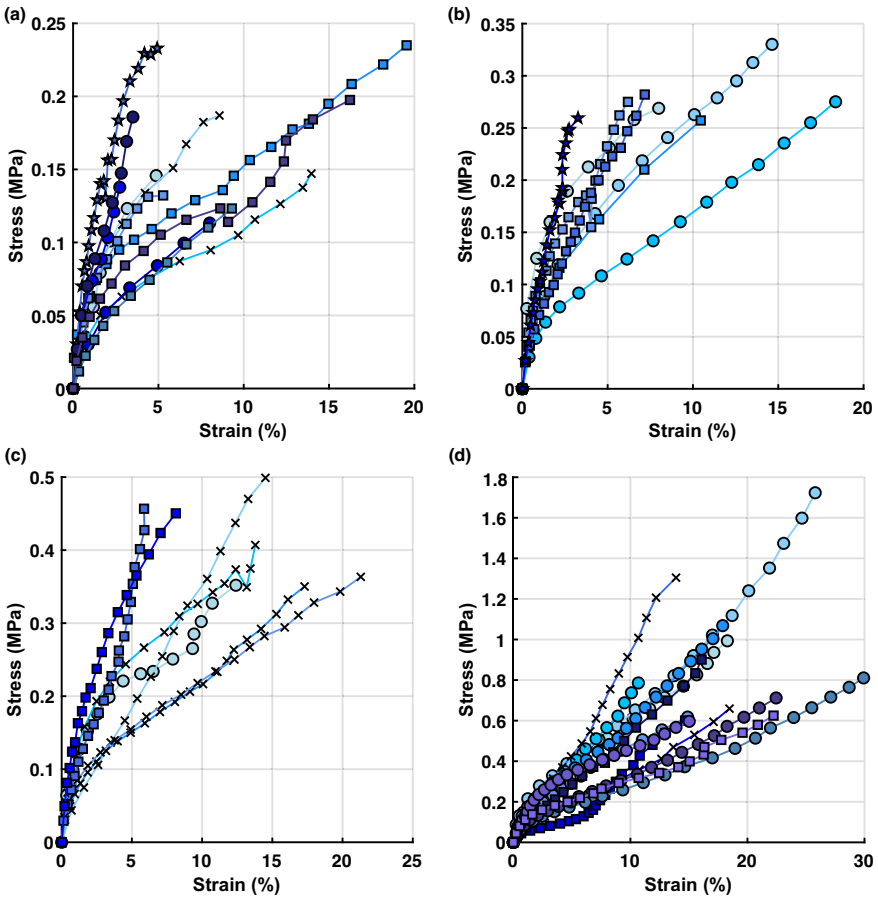

Fig. 6. Stress-strain curves for equine penile and scrotal specimens are presented in four groups based on maximum stress achieved: (a) below 0.25 MPa ($n = 11$), (b) below 0.35 MPa ($n = 9$), (c) below 0.5 MPa ($n = 9$) and (d) below 1.8 MPa ($n = 13$). Data from the free penis portion are denoted in stars, internal lamina in crosses, external lamina in squares, and scrotum in circles. The same colors and symbols are used here and in Fig. 4 to represent the same specimens.

one-way repeated measures ANOVA revealed a significant effect of organ on tangent modulus, with post hoc tests showing significant differences between the vagina and penile sheath ($p = 0.0017$), and between the penile sheath and scrotum ($p = 0.039$), but not between the vagina and scrotum ($p = 0.145$; Fig. 9(d)).

5. Discussion

This is the first experimental study to evaluate and compare the mechanical properties of equine vaginal, penile, and scrotal tissues using uniaxial tensile testing with DIC for strain measurement. The experimental design prioritized high-resolution mechanical characterization by testing a large number of specimens per tissue type under identical conditions. This approach provides strong statistical power for inter-tissue comparisons (vagina, penile sheath, scrotum) and allows robust evaluation of tissue-level mechanical behavior within each organ. Tissues were obtained from two mares and two geldings, and the study therefore examined mechanical differences among genital tissues rather than population-level variability.

The tissue specimens were all loaded along the CD of the vagina, penis, and scrotum, as schematically illustrated in Fig. 1(a)–(e). Our mechanical data show that equine genital tissues are highly nonlinear and inhomogeneous (Figs. 5 and 6), with some variability observed within anatomical regions of the organs (Fig. 9(a)–(b)). The nonlinear response is characteristic of collagenous soft tissues, which initially deform with low stiffness as crimped collagen fibers uncoil. As strain increases, more fibers become aligned and recruited in the loading direction, producing a stiffer response at higher strains. This progressive fiber recruitment explains the nonlinear shape of the stress–strain curves observed across all three tissues. The tangent modulus of the vaginal tissue was higher than the tangent modulus of the penile and scrotal tissues (Fig. 9(d)), indicating that the vagina is stiffer than the penile sheath and scrotum. However, differences in tangent modulus were found to be statistically significant only between the vagina and penile sheath and the penile sheath and the scrotum.

While there are no published studies on the mechanical properties of the equine vagina, several investigators have tested vaginal tissues from other large animal models such as ewes and swine as recently reviewed by Dubik et al. (2025). Our stress–strain and tangent modulus results (Figs. 5 and 9(a)) are comparable with previous data from uniaxial tensile tests on the ewes by Rynkevic et al. (2017). In an earlier study, McGuire et al. (2019) adopted a planar biaxial testing protocol with DIC strain measurements, loading sow vaginal tissue simultaneously in the CD and LD directions to characterize its mechanical behavior. In the CD, biaxially tested swine specimens achieved an average stress of 74 ± 30 kPa at a strain of 15% (McGuire et al., 2019). This is much lower than the stress we measured here, likely due to expected differences in vaginal function across species. Although the vagina consists of a mucosa, muscularis, and adventitia layers in both the mare and sow, the vagina in the mare needs to be stronger and more muscular due to the demands of mating (high-pressure and deep ejaculation from the stallion) and delivery (large foal) (Hammond and Wodzicki, 1941). Previous studies have also mechanically tested human vaginal tissue using uniaxial tensile testing. In cadaveric vaginal tissue, the reported nonlinear stress–strain

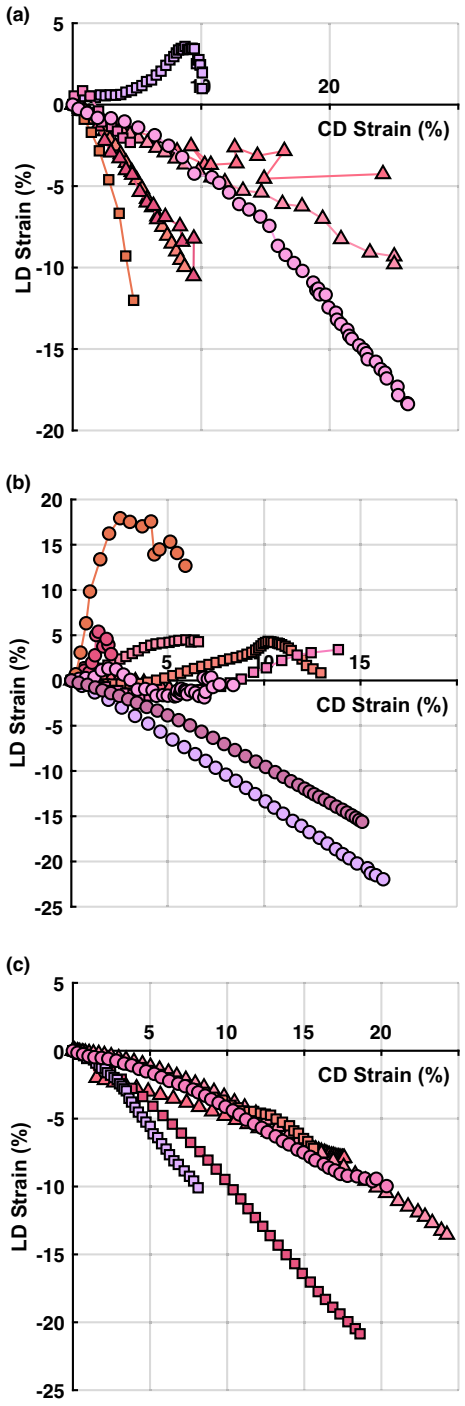

Fig. 7. Transverse (LD)-Axial (CD) strain curves for equine vaginal specimens based on maximum stress achieved: (a) below 1.2 MPa (n = 8), (b) below 1.6 MPa (n = 9), and (c) below 4 MPa (n = 6). Data from proximal, mid, and distal vaginal specimens are denoted by circles, squares, and triangles, respectively. The same colors and symbols are used here and in Figs. 3 and 5 to represent the same specimens.

curves are generally comparable to those observed in the mare (Jean-Charles et al., 2010; Gabriel et al., 2011; Rubod et al., 2012; Chantereau et al., 2014). Although similar stress levels were reached, there were notable differences in strain values due to variations in strain measurement techniques across studies and, naturally, to inherent interspecies anatomical and physiological differences between humans and mares.

Our study is the first to report mechanical properties of both the penile sheath and the scrotum. While previous research has investigated the mechanical behavior of other male genital structures, such as the tunica albuginea and corpus cavernosa in humans and horses (Khorshidi et al., 2024; Bose et al., 2024), the penile sheath and scrotal tissue have not been mechanically characterized until now. We compared our results to those of Bose et al. (2024) and Khorshidi et al. (2024), who used similar testing protocols in equine and human specimens isolated from the corpus cavernosa and the tunica albuginea. Our measured tangent moduli in the CD (i.e., 2.30 ± 1.43 MPa for the penile sheath and 4.81 ± 1.66 MPa for the scrotum) are consistently within the same order of magnitude as the linear region moduli reported in both the CD and LD of the tunica albuginea in both studies. The somewhat lower values observed in our results are expected, as the tunica albuginea plays a central role in supporting intracavernosal pressure during erection, making it a primary load-bearing structure. In contrast, the penile sheath and scrotum are more compliant tissues that serve protective and supportive functions rather than directly resisting internal pressure.

Most specimens experienced a negative strain in the transverse direction (the LD), indicating a reduction in width during uniaxial loading in the CD (Figs. 7 and 8). In a few cases, however, specimens showed a positive transverse strain. This phenomenon has been observed in other soft tissues and is often attributed to fiber reorientation: when fibers within the tissue are not densely packed or fully aligned with the loading direction, they may splay outward, resulting in transverse expansion and a positive strain (Mallett and Arruda, 2017; Luetkemeyer et al., 2020). Although the underlying mechanisms need to be further investigated, positive transverse strain may have a functional role, as genital tissues are designed to expand, deform, and recover to support flexibility, protection, and load distribution during physiological activity.

No statistically significant differences were identified among the proximal, mid, and distal regions of the vagina or the free portion of the penis, internal lamina, and external lamina (Fig. 9(a)–(b)). For the vagina, this outcome contrasts with previously reported findings in human and ovine models (Ulrich et al., 2014; Rynkevic et al., 2017), in which the proximal region of the vagina exhibited greater stiffness (though not significantly greater) than the distal region. These differences may reflect species-specific anatomical or functional variations, or differences in experimental design and testing protocols. One limitation of our study, as well as those cited above, is the small number of specimens analyzed for each anatomical region. Increasing the sample size may allow for more accurate detection and statistical validation of regional differences. Therefore, further work with larger sample sizes is needed to confirm and expand upon these findings.

The mechanical differences observed among the equine vagina, penile sheath, and scrotum offer a comparative framework for understanding how genital tissues resist deformation. Because these tissues serve different physiological functions, their distinct elastic responses provide insight into load-bearing roles, protective mobility, and stretch capacity across genital structures. When comparing the tangent moduli (Fig. 9(d)), vaginal tissue exhibited greater stiffness than scrotal tissue, and both were stiffer than the penile sheath. Notably, no significant difference was found between the vaginal canal and scrotum, suggesting that these tissues share more similar elastic behavior than either does with penile skin. Although species differences are expected, and traction testing cannot be performed *in vivo*, such comparative measurements can inform early-stage engineering design choices and computational modeling of genital tissues. Within this context, the relative similarity between vaginal and scrotal stiffness may be relevant to reconstructive procedures. For example, if analogous relationships hold in humans, scrotal tissue may more closely replicate the elastic behavior of the vaginal wall than penile skin, a consideration relevant to neovaginal construction (Ferrando and Bowers, 2019) and to repairs involving the penile sheath or scrotum. These translational points serve as hypotheses generated from mechanical evidence rather than

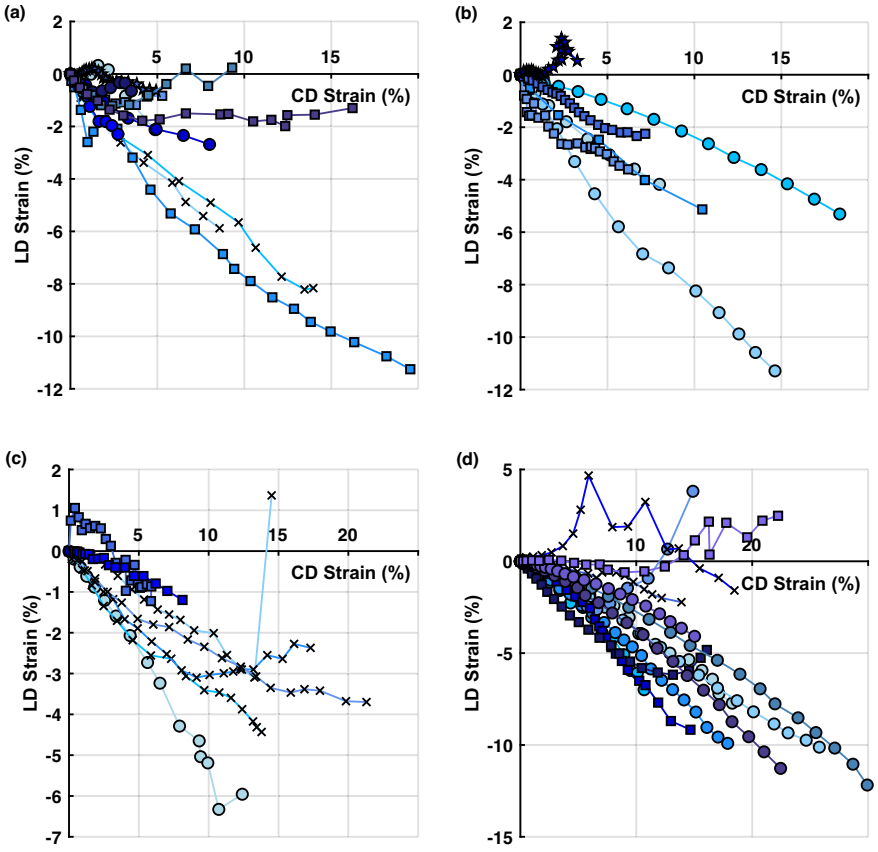

Fig. 8. Transverse (LD)-Axial (CD) strain curves for equine free penis, internal lamina, external lamina, and scrotum specimens presented based on maximum stress achieved: (a) below 0.25 MPa ($n = 11$), (b) below 0.35 MPa ($n = 9$), (c) below 0.5 MPa ($n = 9$) and (d) below 1.8 MPa ($n = 13$). Data from free penis, internal lamina, external lamina, and scrotum specimens are denoted by stars, crosses, squares, and circles, respectively. The same colors and symbols are used here and in Figs. 4 and 6 to represent the same specimens.

direct clinical prescriptions, showing how experimental biomechanics can support long-term improvements in surgical planning and prosthetic design.

This study has limitations that must be discussed. All specimens were loaded uniaxially along the CD, not in the LD. This allowed the specimens to deform freely in the LD, so the mechanical coupling between the two anatomical directions was neglected. Under the assumption of tissue anisotropy, uniaxial tensile testing leads to an oversimplification of the mechanical behavior of the tissues *in vivo*. Building on this uniaxial study, a biaxial study that replicates more physiologically relevant conditions in vaginal, penile, and scrotal tissues would be needed to obtain a complete characterization of the mechanical properties of these tissues. The spread in the load–displacement, stress–strain, and CD and LD strain data (Figs. 3–7) suggests inter-sample variability, which may be attributed to regional tissue differences or other factors such as age and breeding history of the mares and geldings. The specimens included in this study were excised from two mares and two geldings for which detailed veterinary histories were unavailable, potentially introducing mechanical variability. Because the number of animals is limited, this work is not intended to characterize population-level variability. A follow-up study should expand the sample size and incorporate age-matched cohorts, with tissue harvested at defined intervals to represent prepubertal and postpubertal stages, to examine hormonal influences on tissue mechanics. Ideally, each age group would be accompanied by some microstructural imaging to evaluate the architecture of the main components of the tissues. For vaginal specimens from mares, controlling for reproductive history (e.g., maiden vs. foaled) might be crucial for accurately interpreting mechanical behavior, given known differences associated with parity in other animal models (Feola et al., 2010).

Tissue specimens were maintained in a hydrated state during testing by periodically spraying PBS on their surfaces. Although this method helped reduce surface dehydration, it does not replicate the continuous perfusion, nutrient exchange, and biochemical environment of *in vivo* conditions of the vagina, penis, and scrotum. Surface spraying was selected over full immersion to enable accurate speckle tracking and non-contact strain measurement via DIC. In our preliminary testing, maintaining hydration through full immersion compromised speckle pattern adhesion, often leading to speckle loss or movement during testing and affecting the accuracy of strain measurements. Despite our efforts to create and maintain a good speckle pattern throughout the entire testing duration, some specimens experienced significant stretching, compromising the speckle contrast and, therefore, the strain analysis. In some cases, for specimens undergoing very large stretches, the speckles went out of the camera's view, so that the reported strain represents the average only over the region that contained the remaining visible speckles.

Despite some inevitable limitations, the mechanical data obtained in this study can inform the development of material models for computational simulations that account for varied loading conditions, anatomical geometries, and surgical interventions involving genital tissues. These simulations can improve our understanding of genital tissue behavior under physiological and pathological conditions and guide the optimization of surgical techniques and medical device design. This simulation-based approach, based on experimentally obtained mechanical data,

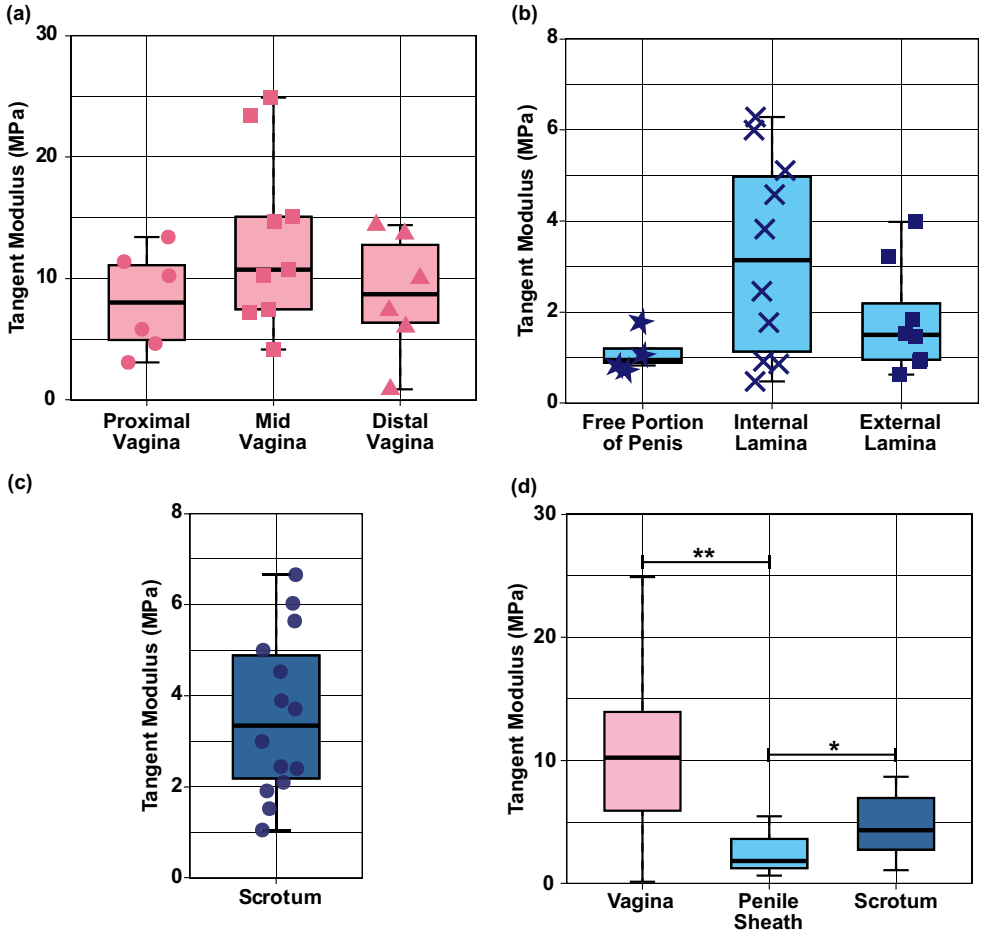

Fig. 9. (a) Boxplot of tangent modulus for the vagina, specifically proximal vagina (circles, $n = 6$), mid vagina (squares, $n = 9$), and distal vagina (triangles, $n = 6$). No statistical difference was detected among anatomical regions ($p \geq 0.1$). Boxplot of tangent modulus for (b) penile sheath, specifically free penis (stars, $n = 4$), internal lamina (crosses, $n = 10$), external lamina (squares, $n = 8$), (c) scrotum (circles, $n = 14$). No statistical difference was detected among the anatomical regions of the penile sheath ($p \geq 0.05$). (d) Boxplot of the tangent modulus for vagina, penile sheath, and scrotum. Statistically significant differences are denoted by * ($p \leq 0.05$) and ** ($p \leq 0.01$).

is particularly valuable given the ethical, practical, and societal constraints associated with collecting biomechanical data from human genital tissues.

6. Conclusions

Our study presents the first mechanical evaluation and comparative analysis of equine vaginal, penile, and scrotal tissues. The collected data demonstrated that these tissues exhibit a nonlinear stress–strain response in the CD and sustain large deformations. Significant differences in tissue stiffness were observed: vaginal tissue was stiffer than scrotal tissue, which in turn was stiffer than penile skin. While these findings require validation in human tissues, they may have important implications for advancing genital reconstructive surgery. The data can help surgeons select graft materials that better replicate the biomechanical properties of the recipient site.

CRediT authorship contribution statement

Angel E. Collins: Writing – review & editing, Writing – original draft, Visualization, Validation, Software, Methodology, Investigation, Formal analysis. **Jennifer S. Wayne:** Writing – review & editing, Writing – original draft, Supervision, Methodology, Investigation. **Cecile A. Ferrando:** Writing – review & editing, Investigation, Conceptualization. **Raffaella De Vita:** Writing – review & editing, Writing – original draft, Visualization, Supervision, Resources, Project administration, Methodology, Investigation, Funding acquisition, Conceptualization.

Declaration of competing interest

The authors declare that they have no known competing financial interests or personal relationships that could have influenced the work reported in this paper.

Acknowledgment

This work was supported by the National Science Foundation under grant # 2135683. The authors would like to thank Dr. Sally Johnson and the Virginia–Maryland College of Veterinary Medicine for their assistance with equine tissue collection.

References

Adams, G.P., Singh, J., Baerwald, A.R., 2012. Large animal models for the study of ovarian follicular dynamics in women. Theriogenology 78, 1733–1748.
Ah-King, M., Barron, A.B., Herberstein, M.E., 2014. Genital evolution: why are females still understudied? PLOS Biol. 12, e1001851.
Alkahtani, D., Mortada, H., Rashidi, M., Al Tamimi, A., 2020. Traumatic degloving injury of penile and scrotal skin: a case report. Plast. Reconstr. Surg.–Glob. Open 8, e3024.
Benammar, A., Derisoud, E., Vialard, F., Palmer, E., Ayoubi, J.M., Poulain, M., Chavatte-Palmer, P., 2021. The mare: a pertinent model for human assisted reproductive technologies? Animals 11, 2304.

Bose, S., Khorshidi, M.A., Johnston, R.D., Watschke, B., Mareena, E., Lally, C., 2024. Experimental testing combined with inverse-FE for mechanical characterisation of penile tissues. Acta Biomater. 179, 180–191.
Budras, K.D., Sack, W.O., Rock, S., Horowitz, A., Berg, R., 2012. Anatomy of the Horse. Schlütersche.
Carnevale, E.M., 2008. The mare model for follicular maturation and reproductive aging in the woman. Theriogenology 69, 23–30.
Chantereau, P., Brieu, M., Kammal, M., Farthmann, J., Gabriel, B., Cosson, M., 2014. Mechanical properties of pelvic soft tissue of young women and impact of aging. Int. Urogynecol. J. 25, 1547–1553.
Dubik, J., Alperin, M., De Vita, R., 2025. The biomechanics of the vagina: a complete review of incomplete data. npj Women's Health 3, 4.
Epstein, L.B., Graham, C.A., Heit, M.H., 2007. Systemic and vaginal biomechanical properties of women with normal vaginal support and pelvic organ prolapse. Am. J. Obstet. Gynecol. 197, 165–e1.
Epstein, L.B., Graham, C.A., Heit, M.H., 2008. Correlation between vaginal stiffness index and pelvic floor disorder quality-of-life scales. Int. Urogynecol. J. 19, 1013–1018.
Feola, A., Abramowitch, S., Jones, K., Stein, S., Moalli, P., 2010. Parity negatively impacts vaginal mechanical properties and collagen structure in rhesus macaques. Am. J. Obstet. Gynecol. 203, 595–e1.
Ferrando, C.A., Bowers, M.L., 2019. Genital gender confirmation surgery for patients assigned male at birth. Comprehensive Care of the Transgender Patient E-Book, Elsevier, Philadelphia, USA, pp. 82.
Foster, R.A., 2016. Male genital system. Jubb Kennedy & Palmer's Pathol. Domest. Anim. 3, 465–510.
Frohrib, D., Goldstein, I., Payton, T.R., Padma-Nathan, H., Krane, R.J., 1987. Characterization of penile erectile states using external computer-based monitoring. J. Biomech. Eng. 109, 110–114.
Gabriel, B., Rubod, C., Brieu, M., Dedet, B., De Landsheere, L., Delmas, V., Cosson, M., 2011. Vagina, abdominal skin, and aponeurosis: do they have similar biomechanical properties? Int. Urogynecol. J. 22, 23–27.
Gefen, A., Chen, J., Elad, D., 1999. Stresses in the normal and diabetic human penis following implantation of an inflatable prosthesis. Med. Biol. Eng. Comput. 37, 625–631.
Gefen, A., Elad, D., Chen, J., 2002. Biomechanical aspects of peyronie's disease in development stages and following reconstructive surgeries. Int. J. Impot. Res. 14, 389–396.
Hammond, J., Wodzicki, K., 1941. Anatomical and histological changes during the oestrous cycle in the mare. Proc. R. Soc. Lond. Ser. B-Biol. Sci. 130, 1–23.
Jean-Charles, C., Rubod, C., Brieu, M., Boukerrou, M., Fasel, J., Cosson, M., 2010. Biomechanical properties of prolapsed or non-prolapsed vaginal tissue: impact on genital prolapse surgery. Int. Urogynecol. J. 21, 1535–1538.
Khorshidi, M.A., Bose, S., Watschke, B., Mareena, E., Lally, C., 2024. Characterisation of human penile tissue properties using experimental testing combined with multi-target inverse finite element modelling. Acta Biomater. 184, 226–238.
de Landsheere, L., Brieu, M., Blacher, S., Munaut, C., Nusgens, B., Rubod, C., Noel, A., Foidart, J.-M., Nisolle, M., Cosson, M., 2016. Elastin density: link between histological and biomechanical properties of vaginal tissue in women with pelvic organ prolapse? Int. Urogynecol. J. 27, 629–635.
Langerhans, R.B., Anderson, C.M., Heinen-Kay, J.L., 2016. Causes and consequences of genital evolution. Integr. Comp. Biol. 56, 741–751.
Lei, L., Song, Y., Chen, R., 2007. Biomechanical properties of prolapsed vaginal tissue in pre-and postmenopausal women. Int. Urogynecol. J. 18, 603–607.
Lionello, G., Sirieix, C., Baleani, M., 2014. An effective procedure to create a speckle pattern on biological soft tissue for digital image correlation measurements. J. Mech. Behav. Biomed. Mater. 39, 1–8.
Lue, T.F., 2000. Erectile dysfunction. N. Engl. J. Med. 342, 1802–1813.
Luetkemeyer, C.M., Rosario, R.A., Estrada, J.B., Arruda, E.M., 2020. Fiber splay precludes the direct identification of ligament material properties: implications for ACL graft selection. J. Biomech. 113, 110104.
Mallett, K.F., Arruda, E.M., 2017. Digital image correlation-aided mechanical characterization of the anteromedial and posterolateral bundles of the anterior cruciate ligament. Acta Biomaterialia 56, 44–57.
McCracken, J.M., Calderon, G.A., Robinson, A.J., Sullivan, C.N., Cosgriff-Hernandez, E., Hakim, J.C.E., 2021. Animal models and alternatives in vaginal research: a comparative review. Reprod. Sci. 28, 1759–1773.
McGuire, J.A., Abramowitch, S.D., Maiti, S., De Vita, R., 2019. Swine vagina under planar biaxial loads: an investigation of large deformations and tears. J. Biomech. Eng. 141, 041003.
McQuillan, S.K., Grover, S.R., 2014. Dilation and surgical management in vaginal agenesis: a systematic review. Int. Urogynecol. J. 25, 299–311.
Pack, E., Dubik, J., Snyder, W., Simon, A., Clark, S., De Vita, R., 2020. Biaxial stress relaxation of vaginal tissue in pubertal gilts. J. Biomech. Eng. 142, 031002.
Rubod, C., Boukerrou, M., Brieu, M., Dubois, P., Cosson, M., 2007. Biomechanical properties of vaginal tissue. Part 1: new experimental protocol. J. Urol. 178, 320–325.
Rubod, C., Brieu, M., Cosson, M., Rivaux, G., Clay, J.-C., de Landsheere, L., Gabriel, B., 2012. Biomechanical properties of human pelvic organs. Urology 79, 968–e17.
Rynkevic, R., Martins, P., Hympanova, L., Almeida, H., Fernandes, A.A., Deprest, J., 2017. Biomechanical and morphological properties of the multiparous ovine vagina and effect of subsequent pregnancy. J. Biomech. 57, 94–102.
Stuntz, M., Perlaky, A., des Vignes, F., Kyriakides, T., Glass, D., 2016. The prevalence of peyronie's disease in the United States: a population-based study. PLoS One 11, e0150157.
Timm, G.W., Wulfman, D.R., Kim, S., Hampton, R.E., Will, S., DiCosimo, J., Erdman, A.G., 2005. Tissue characterization for improved external penile occlusive device design. J. Biomech. Eng. 127, 956–963.
Udelson, D., Nehra, A., Hatzichristou, D.G., Azadzoi, K., Moreland, R.B., Krane, J., Saenz de Tejada, I., Goldstein, I., 1998a. Engineering analysis of penile hemodynamic and structural-dynamic relationships: Part I—clinical implications of penile tissue mechanical properties. Int. J. Impot. Res. 10, 15–24.
Udelson, D., Nehra, A., Hatzichristou, D.G., Azadzoi, K., Moreland, R.B., Krane, R.J., Saenz de Tejada, I., Goldstein, I., 1998b. Engineering analysis of penile hemodynamic and structural-dynamic relationships: Part III—clinical considerations of penile hemodynamic and rigidity erectile responses. Int. J. Impot. Res. 10, 89–99.
Udelson, D., Nehra, A., Hatzichristou, D.G., Azadzoi, K., Moreland, R.B., Krane, R.J., Saenz de Tejada, I., Goldstein, I., 1998c. Engineering analysis of penile hemodynamic and structural-dynamic relationships: Part II—clinical implications of penile buckling. Int. J. Impot. Res. 10, 25–35.
Ulrich, D., Edwards, S.L., Letouzey, V., Su, K., White, J.F., Rosamilia, A., Gargett, C.E., Werkmeister, J.A., 2014. Regional variation in tissue composition and biomechanical properties of postmenopausal ovine and human vagina. PLoS One 9, e104972.
Waites, G.M.H., 1991. Thermoregulation of the Scrotum and Testis: Studies in Animals and Significance for Man. Springer US, Boston, MA, pp. 9–17.